Supporting Information:

A General and Efficient Method for the Site-Specific Dual-Labeling of Proteins for Single Molecule Fluorescence Resonance Energy Transfer

Eric M. Brustad,[‡] Edward A. Lemke, [†,‡] Peter G. Schultz*,[‡] and Ashok A. Deniz*,[†]

[†]*Department of Molecular Biology,* [‡]*Department of Chemistry and the Skaggs Institute for Chemical Biology, The Scripps Research Institute, 10550 North Torrey Pines Road, La Jolla, California 92037*

*Corresponding author. Email: deniz@scripps.edu; schultz@scripps.edu

Methods:

Materials:

p-Acetylphenylalanine was obtained from Synchem (Des Plaines, Illinois). All fluorescent probes were obtained from Molecular Probes (Invitrogen, Carlsbad, CA). 2xYT Media was obtained from BD Biosciences (San Jose, CA) and NiNTA His-Bind® resin was obtained from Novagen (EMD Bioscience, Gibbstown, NJ). All ultra-pure phosphate buffers, sodium chloride, and guanidinium chloride (GdmCl) for labeling and single molecule experiments were obtained from USB Corporation (Cleveland, OH).

ESI-Mass spectrometry:

ESI mass spectrometry was performed on a single-Quad Agilent 1100 series LC-MS with tandem 1100 series ESI mass spectrometer and Chemstations deconvolution software.

Cloning and Mutagenesis:

T4 lysozyme was inserted between the NcoI and KpnI restriction sites of plasmid pBAD-JYAMB4TAG using primers EB78N, EB78C1, and EB78C2 to create plasmid pBAD-JY-T4L. Primers EB78N contains an NcoI site (ccATGg) that orients the ATG start codon of T4 lysozyme. Primers EB78C1 and EB78C2 were used to insert by PCR a 6XHis sequence at the end of the T4 lysozyme gene to facilitate protein purification. Primer EB78C2 also contained a KpnI restriction site for cloning. S38TAG, K83TAG, T157C mutations were constructed by a modified quick change procedure as reported[1] using appropriate primers (see below).

Primer	Sequence
EB78N	tgcattccATGgatatatttgaaatgttacg
EB78C1	gatgtcccgagccacctagatttttatacgcgtccc
EB78C2	gttaaggtacctcaatggtgatggtgatgatgtcccgagccacc
T4L_S38TAGf	agtccaTAGcttaatgctgctaaatctgaattagataaag
T4L_S38TAGr	cattaagCTAtggacttttgtaagcaaatgaccgatgcc
T4L_K83TAGf	gaaatgctTAGttaaaaccggtttatgattctcttgatgc
T4L_K83TAGr	gttttaaCTAagcatttctcagaattccgcgaacagcagc
T4L_T157Cf	ctggcTGTtgggacgcgtataaaaatctaggtggc
T4L_T157Cr	gtcccaACAgccagttctaaacgttgtaatgactcg

Protein Expression:

Plasmid pBAD-JY-T4L contains the T4 lysozyme gene under the control of a araBAD promoter (pBAD), a copy of the araC gene for pBAD expression, a single copy of the *Mj*tRNA$^{Tyr}_{CUA}$ under the control of a constitutive LPP promoter, a low copy p15A origin, and a tetracycline resistance gene for plasmid maintenance. For unnatural amino acid expression, pBAD-JY-T4L TAG mutants were cotransformed with plasmid pBK-

*p*AcPheRS, which contains the orthogonal *p*-acetylphenylalanine (**1**) tRNA synthetase under the control of the constitutive Gln promoter, a high copy pMB1 origin, and a kanamycin resistance marker for plasmid maintenance. 5 mL starter cultures were used to inoculate 2 L 2xYT supplemented with 1 mM of **1,** 50 μg/mL kanamycin and 25 μg/mL tetracycline. Cells were grown at 37 ºC until they reached an OD_{600} of 0.5 at which time 0.02% arabinose was added to induce protein expression. Cultures were shifted to 30 ºC and grown an additional 16 hrs. Cells were harvested, lysed and T4 lysozyme was purified on Ni-NTA resin using standard procedures. T4 lysozyme was then exchanged into 50 mM MES buffer, pH 6.3, 50 mM NaCl, 1 mM EDTA and purified to homogeneity on a monoS 5/5 column (GE Life Sciences) using a gradient from 50 mM NaCl to 500 mM NaCl. T4 lysozyme typically eluted around 275 mM NaCl.

Circular dichroism of T4 lysozyme mutants:

Purified wildtype T4L* and ketone/cysteine mutants were exchanged into 50 mM sodium phosphate buffer, pH 7.5, 150 mM NaCl, and concentrated to 100 μM to provide 10X stocks for CD experiments. The protein was diluted to a final concentration of 10 μM into buffer to which an appropriate amount of denaturant was added from an 8 M GdmCl stock (50 mM sodium phosphate buffer, pH 7.5, 150 mM NaCl, 8M GdmCl). 300 μL of each protein solution was loaded into a 2 mm quartz cuvette (Hellma QC) and CD spectra were obtained on an AVIV 202SF CD spectropolarimeter.

At each denaturant concentration, CD spectra were taken in triplicate between 270 nm and 215 nm in 1 nm increments with a 2 second integration time. Data were averaged and background spectra from free buffer solutions were subtracted. CD values at 222 nm were plotted versus denaturant concentration to provide denaturation curves for the unlabeled proteins (figure S5).

Fluorescent labeling of ketone amino acid (1):

Oxime formation between **1** with Alexa488-alkoxyamine shows a pH dependence with optimum labeling occurring at pH 4.0 (50 mM sodium acetate, pH 4.0, 150 mM NaCl), consistent with acid catalyzed oxime formation (figure S1a). Lower labeling yields are observed at > pH 5; however, others have shown that the rate of labeling can be increased at physiological pH through the use of appropriate aniline catalysts.[2] Reactions performed at 100 μM or greater protein concentration typically gave > 90 % labeling after 12 hrs reaction at 37 ºC. Labeling reactions performed at less than 50 μM protein concentration are kinetically slow and show a significant decrease in yield (figure S1b) using the 12 hours labeling conditions. Reactions on lower concentrations of protein can be accelerated by the use of aniline catalysts, which may be necessary for more sensitive protein samples.[2] Yields were determined by comparing absorbance at 494 nm (Alexa 488 $\varepsilon_{494} = 72{,}000\ M^{-1}cm^{-1}$) with the protein absorbance at 280 nm (T4L* $\varepsilon_{280} \sim 26{,}000\ M^{-1}cm^{-1}$) after subtracting the Alexa488 contribution at 280 nm (0.15 times the absorbance at 494).

In a typical labeling experiment, ketone containing protein is exchanged into pH 4.0 alkoxyamine labeling buffer (50 mM sodium acetate, pH 4.0, 150 mM NaCl) and

then concentrated to a final concentration of 100 μM using a 10 kDa cutoff Amicon® Ultra Centrifugal Filtration Device (Millipore, Billerica, MA). Five equivalents of Alexa488-alkoxyamine are then added and the reaction is incubated overnight at 37 ºC. Excess unreacted dye is then removed by desalting on a PD10 desalting column (GE Life Sciences) followed by washing using 3X 100 fold dilutions with 50 mM sodium phosphate buffer, pH 7.5, 150 mM NaCl, 6M GdmCl in a 10 kDa cutoff 5 mL Amicon® Ultra Centrifugal Filtration Device.

*Double labeling of keto(**1**)/Cys mutants:*

Purified T4L* keto(**1**)/Cys double mutants were exchanged into 50 mM sodium phosphate buffer, pH 7.5, 150 mM NaCl, supplemented with 1 mM dithiothreitol (DTT) to reduce any undesired disulfide bonds that may have formed during the purification procedure. Proteins were then buffer exchanged into maleimide labeling buffer (50 mM sodium phosphate buffer, pH 7.5, 150 mM NaCl, 6 M GdmCl) by washing 3X 100 fold dilutions using a 10 kDa cutoff 5 mL Amicon® Ultra Centrifugal Filtration Device to remove excess DTT. Five equivalents of Alexa594-maleimide were then added to label the free cysteine thiol at room temperature for 5 hrs. Excess unreacted dye was removed by either dialysis against 50 mM sodium phosphate buffer, pH 7.5, 150 mM NaCl or washing on Ni-NTA immobilized protein after which the protein was exchanged into pH 4 ketone labeling buffer. 5-10 equivalents of Alexa488-alkoxyamine were then added and the reaction was allowed to proceed at 37 ºC overnight. Excess dye was then removed by exhaustive dialysis against water. Protein was aliquoted and lyophilized to dryness for easy storage.

Single-molecule FRET:

Single molecule FRET experiments were performed as previously described.[3] Briefly, laser light at 488 nm from an argon ion laser (Melles Griot, Carlsbad, CA) was coupled into a Zeiss Axiovert 200 microscope (Zeiss, Thornwood, NY) by a single mode fiber (Pointsource, Hamble, UK) and focused into the sample using a Zeiss C-Apochromat 40x, 1.2 NA, after passing a λ/4 plate. The emitted light was separated from the excitation light using a dichroic beam splitter (Q495LP, Chroma Tech. Corp., Rockingham, VT) and further spatially filtered by focusing on a 100 μm pinhole. The light was spectrally split into Donor and Acceptor channels using another dichroic beam splitter (DC560, Chroma). After passing through a bandpass filter in the Donor channel (525/50, Chroma) and a 590LP (Chroma) in the acceptor channel, the light was focused onto avalanche photon counting modules (SPCM-AQR-14, Perkin-Elmer Optoelectronics, Fremont, CA). An SPC630 card operating (Becker&Hickl, Berlin, Germany) in the FIFO TAG mode was used to detect the arrival time of the individual photons. Individual bursts were identified using a previously described burst search algorithm[4] and resulting FRET histogram analysis was done using IgorPro (Wavemetrics, Lake Oswego, OR) after threshholding the data at 50 counts per burst. The correction values for spectral bleed through (*L)* and direct excitation (*D*) were determined from control experiments and the absorption and emission spectra of the dyes to be 0.07 and 0.03 respectively.

The measured photon signals (R_D and R_A) include the crosstalk components due to D and L and are related to the corrected photon signals I_D and I_A as follows:

$$R_D = I_D * (1 - L) \qquad \textbf{[S1]}$$
$$R_A = L * I_D + I_A + D * (I_D + I_A)$$

Solving for I_D and I_A yields:

$$I_D = -\frac{R_D}{L-1} \qquad \textbf{[S2]}$$
$$I_A = \frac{R_A - L * R_A - L * R_D - D * R_D}{1 + D - L - L * D}$$

Gaussian fits of corresponding histograms were calculated using IGOR software and the peak position was obtained from the fitting parameters. Contour plots of T4L* unfolding were created using Origin (OriginLab Corp., Northampton, MA).

Single molecule protein denaturation experiments:

Individual double-labeled T4L* aliquots were brought back into solution using 50 mM sodium phosphate buffer, pH 7.5, 150 mM NaCl, supplemented with 6 M GdmCl and the protein concentration was adjusted to approximately 20 μM. Prior to single molecule experiments, proteins were diluted 2000-fold into refolding buffer (50 mM sodium phosphate buffer, pH 7.5, 150 mM NaCl) to create a 10 nM (100X) protein stock which was allowed to refold for a minimum of 2 hours on ice prior to single molecule experiments. Protein was diluted 100 fold (~100 pM) into each final denaturant concentration and, after 10 minutes of equilibration, single molecule data were collected as described above. The final GdmCl concentration was obtained by diluting an 8M GdmCl solution (50 mM sodium phosphate buffer, pH 7.5, 150 mM NaCl, 8M GdmCl) with the appropriate amount of refolding buffer.

Determining the effect of denaturant on the photophysical properties of donor and acceptor fluorophores: Contributions of gamma (γ)

FRET efficiencies (E_{FRET}) were ratiometrically determined based on the equation

$$E_{FRET} = \frac{I_A}{I_A + \gamma I_D} \qquad \textbf{[S3]}$$

where I_A and I_D are the corrected acceptor and donor photon signals respectively (Equations **S2**). γ is a correction factor dependent on the quantum yields of both fluorophores (Φ_A and Φ_D) as well as the detection efficiency of the donor channel (η_D) and acceptor channel (η_A) of the single-molecule setup.

$$\gamma = \frac{\eta_A \Phi_A}{\eta_D \Phi_D} \qquad \textbf{[S4]}$$

γ can be simplified on the basis of instrument properties (η_D and η_A) and dye properties (Φ_A and Φ_D) to yield the expression

$$\gamma = \gamma_{Instrument}\gamma_{System} \quad \textbf{[S5]}$$

where $\gamma_{Instrument} = \eta_A/\eta_D$ and $\gamma_{System} = \Phi_A/\Phi_D$.

$\gamma_{Instrument}$ was determined to be 1.4 by measuring the fluorescence of free donor and acceptor dyes as functions of dye concentration in refolding buffer, using both an ensemble spectrofluorometer and the single-molecule setup described above. $\gamma_{Instrument}$ was calculated from

$$\gamma_{Instrument} = \frac{m_D^{eF}}{m_D^{smF}} \frac{m_A^{smF}}{m_A^{eF}} \quad \textbf{[S6]}$$

where m_D^{eF} and m_A^{eF} are the dye concentration-dependent slopes of donor and acceptor integrated ensemble fluorescence intensities and m_D^{smF} and m_A^{smF} are the dye concentration-dependent slopes of donor and acceptor single-molecule fluorescence intensities.

Dye quantum yields were determined by the comparative method of Williams *et al.*[5] where a reference standard is used to calculate the quantum yields of both donor and acceptor fluorophores. Fluorescein was used as a reference dye for the determination of Alexa 488 quantum efficiency while cresyl violet was used to determine the quantum efficiency or the Alexa 594 acceptor fluorophore. Briefly, absorbance and fluorescence measurements were performed for the reference standards and the experimental samples (x) at different concentrations. Slopes from linear plots of absorbance (m^A) and integrated fluorescence intensity (m^F) versus concentration were determined, and then used to calculate sample quantum yields (Φ_X) using the equation

$$\Phi_X = \Phi_{ref} \frac{m_x^F}{m_x^A} \frac{m_{ref}^A}{m_{ref}^F} \frac{n_x^2}{n_{ref}^2} \quad \textbf{[S7]}$$

where Φ_{ref} is the reported absolute quantum yield for the standard, and n_x and n_{ref} are the solvent refractive indices for the sample and the standard, respectively.

Fluorescein has a quantum yield of 0.95 in 100 mM NaOH (n = 1.334) and an excitation range from 471-475 nm was used to give a complete fluorescence spectrum. The quantum yield for cresyl violet is 0.54 in methanol (n = 1.329) and an excitation range 548 – 552 nm was used. These excitation ranges were also used for both donor and acceptor dye γ measurements.

This method was used to assess the effect of GdmCl on the photophysical properties of fluorescently labeled T4L mutants. The quantum yield of each dye was determined on acceptor-only or donor-only labeled T4L*S38(**1**)/T157C protein at a variety of denaturant concentrations. The addition of GdmCl has significant impact on the buffer refractive index; as such, n was determined at room temperature using an Abbe 3L refractometer (Spectronic Instruments) prior to each experiment. The determined quantum yields and γ values are summarized in Table S1. The effect of γ on the denaturant dependent peak shift of the T4L*S38(**1**)/T157C native state is shown in Table S2 and figures S4a and S4b.

Interdye Distance Determination:

Interdye distance can be calculated from the observed FRET efficiencies by

$$E_{FRET} = \frac{R_0^6}{(R_0^6 + r^6)} = \frac{1}{1 + \left(\frac{r}{R_0}\right)^6} \qquad \textbf{[S8]}$$

where r is the interdye distance and R_0 is the Förster distance for a given donor-acceptor dye pair. R_0 is given by

$$R_0 = 0.211[\kappa^2 n^{-4} \Phi_D J(\lambda)]^{1/6} \qquad \text{(in Å)} \qquad \textbf{[S9]}$$

where κ^2 is the orientation factor, usually assumed to be 2/3 for dyes with dynamically averaged orientation. Given the relatively low values of steady-state fluorescence polarization anisotropy measured vs. denaturant for both donor and acceptor dyes (Table S1) this $\kappa^2 = 2/3$ assumption is reasonable as applied to this work. $J(\lambda)$ is the overlap integral described by

$$J(\lambda) = \int_0^\infty F_D(\lambda)\varepsilon_A(\lambda)\lambda^4 \partial\lambda \qquad \text{(in } M^{-1}cm^{-1}nm^4\text{)} \qquad \textbf{[S10]}$$

$F_D(\lambda)$ is the corrected donor fluorescence intensity at wavelength λ (area normalized to unity; dimensionless), and $\varepsilon_A(\lambda)$ is the acceptor extinction coefficient at wavelength λ (in $M^{-1}cm^{-1}$). λ is in nm.

From Eqs. **S3** and **S8**,

$$r = \left(\frac{1}{E_{apparent}} - 1\right)^{1/6} R_0 \gamma^{1/6} \qquad \textbf{[S11]}$$

where $E_{apparent}$ is the experimentally determined FRET efficiency, i.e., $\left(\frac{I_A}{I_A + I_D}\right)$.

The Förster distance (R_0) was calculated as described in equations **S9** and **S10** by using fluorescence and absorbance spectra of singly donor and acceptor labeled T4L*S38(**1**)/T157C at various GdmCl concentrations. Interdye distances at each denaturant concentration were determined by applying equation **S11** using these values of R_0 in addition to the calculated γ values summarized in table S1. The interdye distance results are also summarized table S1.

Effects of denaturant on E_{FRET} shifts in the native state:

As shown in figure S4 and summarized in tables S1 and S2, effects of denaturant on the γ correction factor do not significantly affect the large shift in E_{FRET} observed in the native state of T4L*S38(**1**)/T157C. In fact, the shift becomes even more pronounced when including γ in ratiometric E_{FRET} calculations as well as calculations of interdye distance. In total, a decrease in E_{FRET} of 0.21 (from 0.69 at 0 M GdmCl to 0.48 at 1.4 M GdmCl) is observed prior to the cooperative unfolding transition of T4 lysozyme under these conditions. This shift corresponds to an increase in interdye distance of approximately 8 Å and may be indicative of a significant change in the overall native state protein structure prior to global unfolding. Further study is required to elucidate the nature of this effect.

Potential errors in distance measurements:

In smFRET experiments, several factors contribute to errors in absolute distance measurements, including uncertainties in the orientation factor κ^2, dye linker length and dynamics, and statistical noise. For a more detailed discussion of error sources, we refer the reader to previous literature.[6-8] In particular, the potentially major contributor to the error in absolute distance measurement is the assumption of $\kappa^2 = 2/3$. It has recently been estimated that in extreme cases where this assumption is not justified, particularly if the dye transition moments are close to perpendicular to each other, the error in the distance estimate could be up to 12 Å.[9] However, our anisotropy values are moderately low (< 0.15); hence we can assume that the dyes are reasonably mobile and the error in the absolute distance estimate is much lower than 12 Å. This is further validated given that our distance estimates match the distance observed in the crystal structures.

Supporting Figures:

Figure S1.

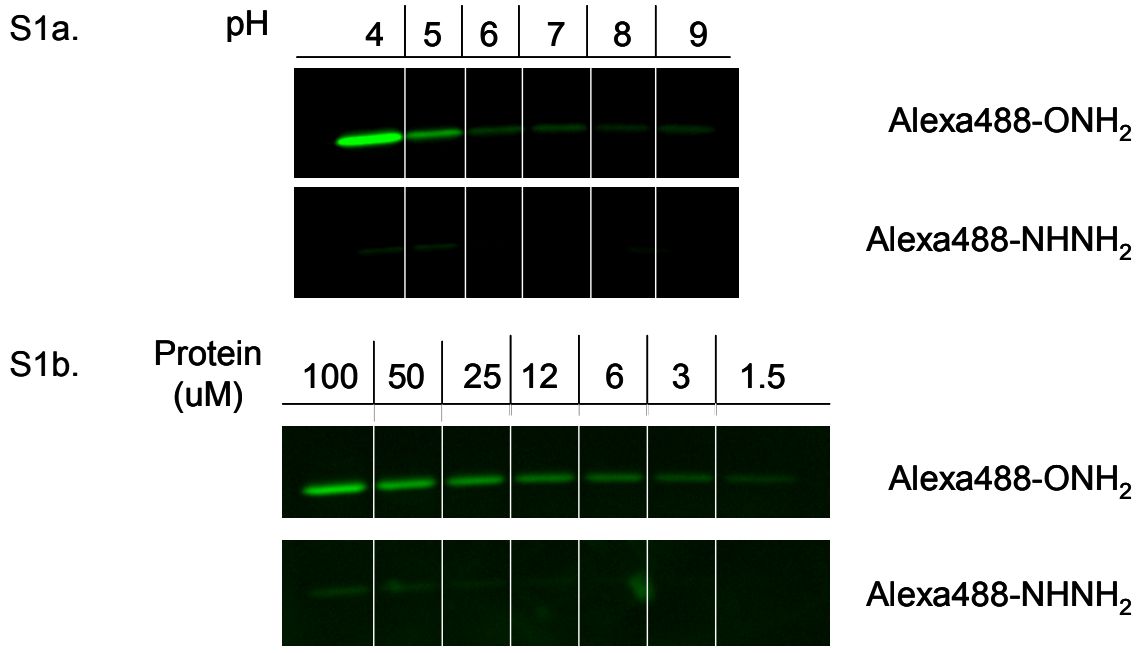

Figure S1a: Ketone(1) labeling with alkoxyamino and hydrazide dyes.
100 μM T4 lysozyme D72**(1)** was labeled in the presence of 1 mM Alexa-488 dye at 37 °C for 24 hrs at the indicated pH. After labeling, protein were separated by SDS-PAGE and fluorescence was imaged using a Storm 420 Phosphoimager in the blue fluorescence mode. Buffer composition: pH 4: 50 mM sodium acetate, 150 mM NaCl; pH 5: 50 mM sodium acetate, 150 mM NaCl; pH 6: 50 mM sodium phosphate, 150 mM NaCl; pH 7: 50 mM sodium phosphate, 150 mM NaCl; pH 8: 50 mM CHES buffer, 150 mM NaCl; pH 9: 50 mM CAPS buffer, 150 mM NaCl

Figure S1b: Dependence of labeling yield on protein concentration
Serial dilutions of T4 lysozyme D72**(1)** at the indicated concentrations were incubated with a 10X equivalent of either Alexa488 hydroxylamine or Alexa488 hydrazide dyes in 50 mM NaOAc, pH 4.0, 150 mM NaCl buffer. After 12 hrs incubation at 37 °C, proteins were normalized to a final concentration of 1.5 μM and separated by SDS-PAGE. Fluorescence was imaged using a Storm 420 Phosphoimager in the blue fluorescence mode.

Figure S2: ESI analysis of T4 lysozyme labeling reactions

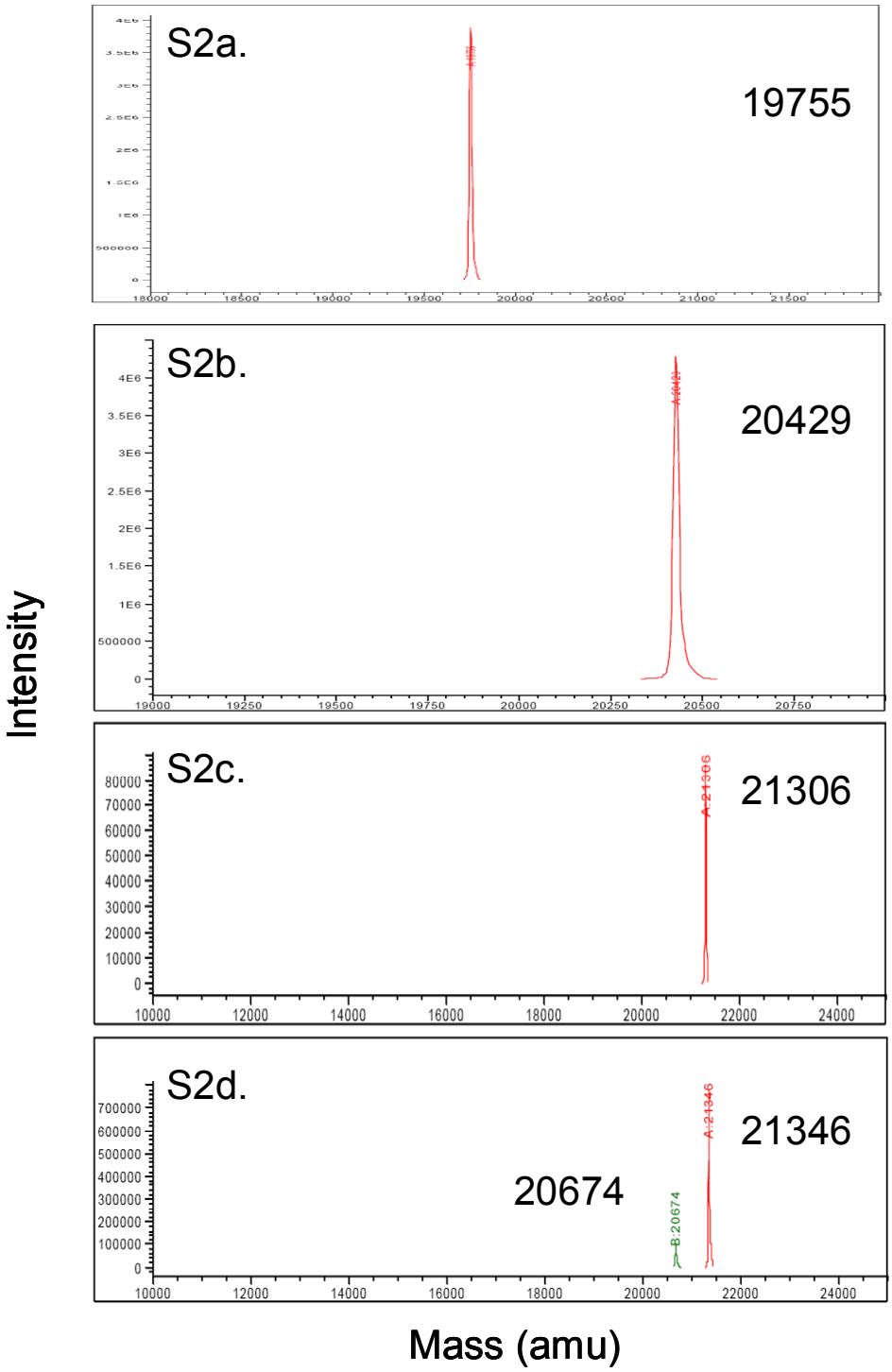

Figure S2a:
Unlabeled T4 lysozyme D72**(1)** shows a single peak corresponding to T4 lysozyme with the ketone amino acid (**1**) at position 72.
Calcd: 19757 (M + H)
Obsd: 19755

Figure S2b:
T4 lysozyme D72**(1)** after 12 hours labeling with Alexa-488 alkoxyamine. Deconvoluted ESI shows a single peak corresponding to the T4 lysozyme-Alexa488 conjugated oxime product.
Calcd: 20430 (M+H)
Obsd: 20429

Figure S2c:
T4 lysozyme K83**(1)**/T157C was labeled with Alexa594 maleimide and Alexa488 hydroxylamine as described in the methods section. Protein was analyzed by LCMS/ESI mass spectrometry.
Calcd. 21307 (M + H)
Obsd. 21306

Figure S2d:
T4 lysozyme S38**(1)**/T157C was labeled with Alexa594 maleimide and Alexa488 hydroxylamine as described in the experimental section. Protein was analyzed by LCMS/ESI mass spectrometry.
Double labeled: calcd. 21347, obsd, 21346
Alexa594 Maleimide single labeled: calcd. 20675, obsd. 20674.

*Figure S3: smFRET data for T4L*S38(**1**)/T157C*

S3a.

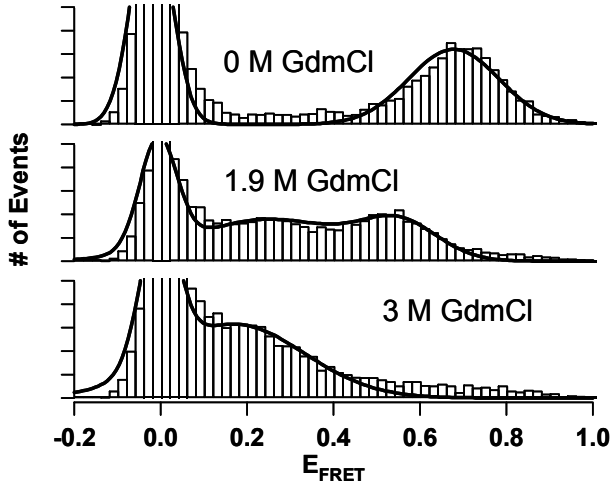

S3b.

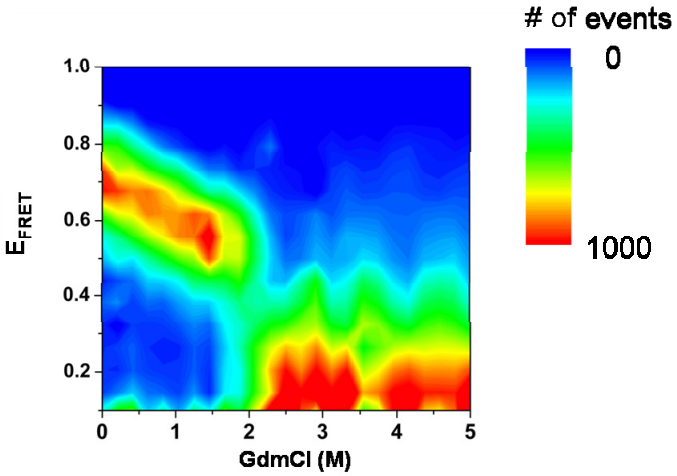

Figure S3a:
Sample smFRET histograms for double-labeled T4L*S38(**1**)/T157C. The peak centered around zero E_{FRET} (highlighted in grey) is the result of incomplete labeling or photobleached or otherwise nonfluorescent Alexa 594 maleimide dye.

Figure S3b:
Contour plot of double-labeled T4L*S38(**1**)/T157C unfolding reaction assembled from smFRET histograms. Numbers of events are shown by a color spectrum ranging from high (red) to low (blue). The decrease in E_{FRET} for the native state prior to the cooperative unfolding transition is clearly visible in this plot.

*Table S1: Effect of GdmCl on dye properties of labeled T4L*S38(**1**)/T157C, R_0, and interdye distances (r)*

GdmCl (M)	Donor anisotropy	Acceptor anisotropy	$\Phi_{Donor\text{-}Labeled}$	$\Phi_{Acceptor\text{-}Labeled}$	γ *system*	γ	R_0 (Å)	r (Å)
0	0.15	0.14	0.32	0.21	0.66	0.93	46.9	40.9
0.6	0.14	0.13	0.29	0.22	0.76	1.06	47.1	44.1
1	0.13	0.11	0.33	0.29	0.86	1.21	49.2	48.3
1.4	0.13	0.10	0.28	0.25	0.86	1.21	48.4	49.0
3	0.09	0.08	0.28	0.37	1.35	1.89	48.3	69.3

Table S2: Effect of γ on observed E_{FRET}[a,b]

GdmCl (M)	E_{FRET} (uncorrected)	E_{FRET} (γ corrected)
0	0.68	0.69
0.6	0.61	0.60
1	0.58	0.53
1.4	0.53	0.48
3	0.18	0.10

a. uncorrected E_{FRET} values were calculated using equation S1 and an assumed γ parameter of 1 (also call $E_{apparent}$).
b. corrected E_{FRET} values were calculated using equation S1 and the γ values summarized in table S1

Figure S4: Effects of γ on observed E_{FRET}

S4a.

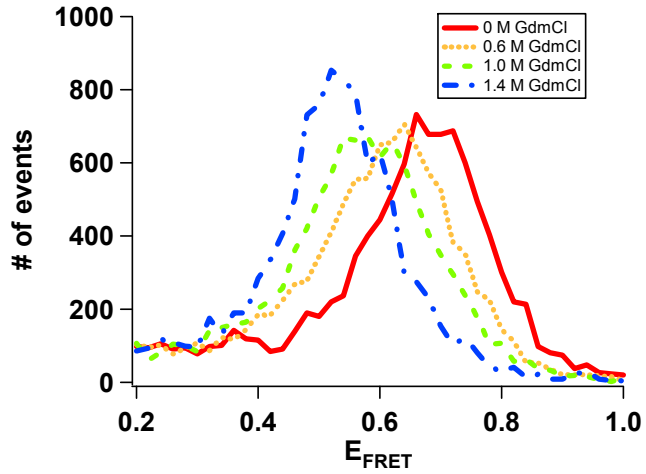

S4b.

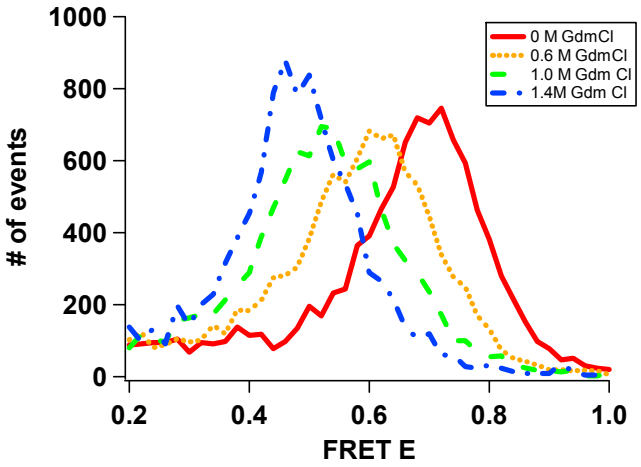

Figure S4a:
Uncorrected E_{FRET} values for folded double labeled T4L*S38(**1**)/T157C at various denaturant concentrations

Figure S4b:
E_{FRET} for folded double labeled T4L*S38(**1**)/T157C at various denaturant concentrations corrected with contributions from γ parameter.

Figure S5: Protein unfolding curves of T4 lysozyme variants.

Protein	T4L* Wildtype	T4L*S38(1) /T157C	T4L*K83(1)/ T157C	T4L*K83(1)/T157C smFRET data
ΔG^0 (Kcal/mol)	-13.4 +/- 0.9	-11.68 +/- 0.8	-10 +/- 0.7	-10.5 +/- 1.1

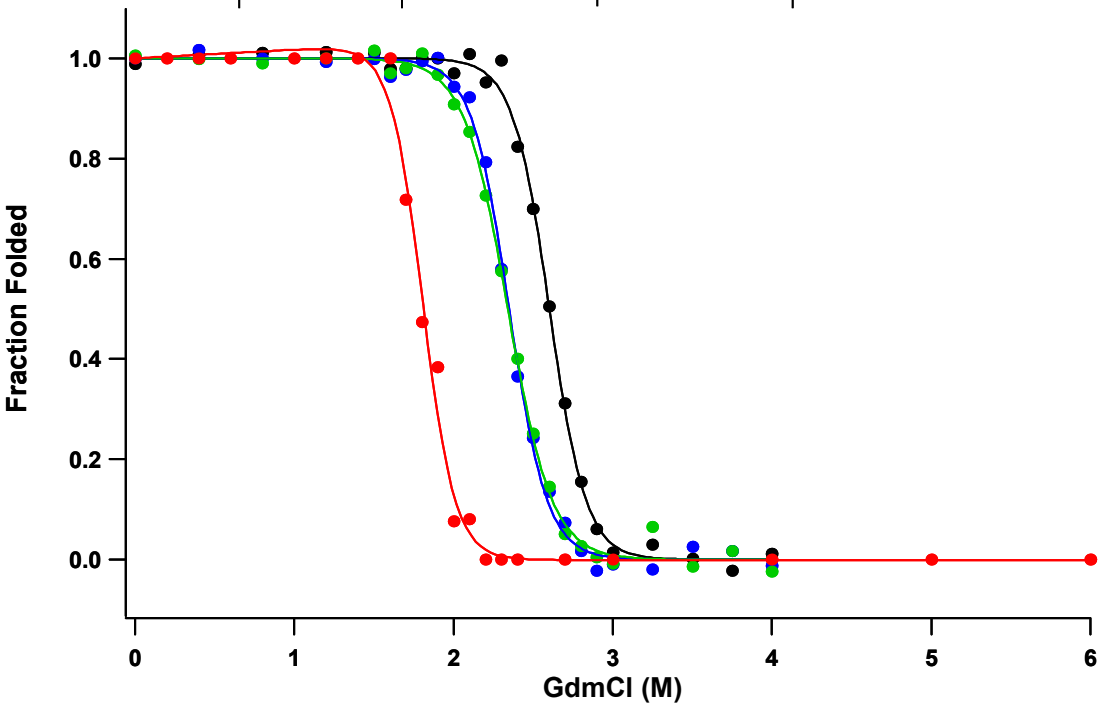

CD unfolding curves: wildtype (black), unlabeled T4L*38(1)/157Cys (blue), and unlabeled T4L*83(1)/157Cys (green). Unfolding of double labeled T4L*83(1)/157Cys as determined by smFRET is also shown (red)

To ensure that the presence of a 6xHis tag does not affect the stability of T4L*, circular dichroism was used to observe the folding of His-tagged wild-type and mutant T4L* using GdmCl as a denaturant. Unfolding curves of CD 222 nm vs. GdmCl were fit via the method of Bolen *et al.*[10,11] and the fraction folded at each denaturant concentration was calculated from these fits and plotted above. Stability of 6xHis tagged wt T4L* was consistent with previous reports suggesting that the His tag does not significantly affect T4 lysozyme stability.[12,13] Double mutants are slightly destabilized compared to the wild-type protein, stressing the need for appropriate controls when performing single molecule experiments.

Unfolding curves obtained from single molecule FRET demonstrated cooperative unfolding consistent with what is known for this protein under equilibrium conditions; however, dual-labeled protein showed some destabilization due to the presence of the fluorophores. As a general strategy, it may be useful to screen other fluorophore scaffolds (e.g. Alexa, Atto, or cyanine dyes) to find pairs that minimize these effects.

Figure S6: Final T4 lysozyme protein sequences.
It should be noted that Asn2 was mutated to D to facilitate cloning. Analysis of the crystal structure suggested that this mutation would not affect the protein structure significantly. This is supported by CD unfolding data which shows a similar unfolding transition to previous reports (figure S5).[12,13]

X = Ketone amino acid (**1**)

T4L D72**(1)**
MDIFEMLRIDEGLRLKIYKDTEGYYTIGIGHLLTKSPSLNAAKSELDKAIGRNTNG
VITKDEAEKLFNQDV**X**AAVRGILRNAKLKPVYDSLDAVRRAALINMVFQMGET
G VAGFTNSLRMLQQKRWDEAAVNLAKSRWYN QTPNRAKRVITTFRTGTWDA
YKNLGGSGHHHHHH

T4 Lysozyme S38**(1)**/T157C:
MDIFEMLRIDEGLRLKIYKDTEGYYTIGIGHLLTKSP**X**LNAAKSELDKAIGRNTNG
VITKDEAEKLFNQDVDAAVRGILRNAKLKPVYDSLDAVRRAALINMVFQMGET
GVAGFTNSLRMLQQKRWDEAAVNLAKSRWYNQTPNRAKRVITTFRTG**C**WDAY
KNLGGSGHHHHHH

T4 Lysozyme K83**(1)**/T157C:
MDIFEMLRIDEGLRLKIYKDTEGYYTIGIGHLLTKSPSLNAAKSELDKAIGRNTNG
VITKDEAEKLFNQDVDAAVRGILRNA**X**LKPVYDSLDAVRRAALINMVFQMGET
GVAGFTNSLRMLQQKRWDEAAVNLAKSRWYNQTPNRAKRVITTFRTG**C**WDAY
KNLGGSGHHHHHH

References:

(1) Zheng, L.; Baumann, U.; Reymond, J. L. *Nucleic Acids Research* **2004**, *32*, 5.
(2) Dirksen A., H. T. M. D. P. E. *Angewandte Chemie* **2006**, *118*, 7743-7746.
(3) Mukhopadhyay, S.; Krishnan, R.; Lemke, E. A.; Lindquist, S.; Deniz, A. A. *Proceedings of the National Academy of Sciences of the United States of America* **2007**, *104*, 2649-2654.
(4) Eggeling, C.; Berger, S.; Brand, L.; Fries, J. R.; Schaffer, J.; Volkmer, A.; Seidel, C. A. M. *Journal of Biotechnology* **2001**, *86*, 163-180.
(5) Williams, A. T. R.; Winfield, S. A.; Miller, J. N. *Analyst* **1983**, *108*, 1067-1071.
(6) Deniz, A. A.; Laurence, T. A.; Beligere, G. S.; Dahan, M.; Martin, A. B.; Chemla, D. S.; Dawson, P. E.; Schultz, P. G.; Weiss, S. *Proceedings of the National Academy of Sciences of the United States of America* **2000**, *97*, 5179-5184.
(7) Deniz, A. A.; Dahan, M.; Grunwell, J. R.; Ha, T. J.; Faulhaber, A. E.; Chemla, D. S.; Weiss, S.; Schultz, P. G. 1999, p 3670-3675.

(8) Deniz, A. A.; Laurence, T. A.; Dahan, M.; Chemla, D. S.; Schultz, P. G.; Weiss, S. *Annual Review of Physical Chemistry* **2001**, *52*, 233-253.
(9) Iqbal, A.; Arslan, S.; Okumus, B.; Wilson, T. J.; Giraud, G.; Norman, D. G.; Ha, T.; Lilley, D. M. J. *Proceedings of the National Academy of Sciences of the United States of America* **2008**, *105*, 11176-11181.
(10) Bolen, D. W.; Santoro, M. M. *Biochemistry* **1988**, *27*, 8069-8074.
(11) Santoro, M. M.; Bolen, D. W. *Biochemistry* **1988**, *27*, 8063-8068.
(12) Cellitti, J.; Bernstein, R.; Marqusee, S. *Protein Science* **2007**, *16*, 852-862.
(13) Llinas, M.; Gillespie, B.; Dahlquist, F. W.; Marqusee, S. *Nature Structural Biology* **1999**, *6*, 1072-1078.